DESIGN AND DEVELOPMENT OF SPLIT-RING RESONATOR-BASED SENSORS FOR DIELECTRIC CONSTANT MEASUREMENT

OH ZI XIN

MASTER OF ENGINEERING SCIENCE

FACULTY OF ENGINEERING AND GREEN TECHNOLOGY
UNIVERSITI TUNKU ABDUL RAHMAN
NOVEMBER 2022

DESIGN AND DEVELOPMENT OF SPLIT-RING RESONATOR-BASED SENSORS FOR DIELECTRIC CONSTANT MEASUREMENT

By

OH ZI XIN

A dissertation submitted to the Department of Electronic Engineering,
Faculty of Engineering and Green Technology,
Universiti Tunku Abdul Rahman,
in partial fulfillment of the requirements for the degree of
Master of Engineering Science
November 2022

ABSTRACT

DESIGN AND DEVELOPMENT OF SPLIT-RING RESONATOR-BASED SENSORS FOR DIELECTRIC CONSTANT MEASUREMENT

Oh Zi Xin

Dielectric constant measurement is an important topic in electronic circuit design. In this study, circular and square SRR-based sensors are proposed to overcome the limitations of conventional measurement methods. Both SRR-based sensors loaded a quarter wavelength coplanar waveguide (CPW) transmission line with two ports and have a size of 35 mm x 35 mm x 1.27 mm. The transmission coefficient is used as the measurement parameter. S21 resonance shifts when material under test (MUT) is put on top of SRR. The proposed circular and square SRR sensors are fabricated at Rogers RO3210 substrate material with a relative permittivity of 10.2. The resonance frequency of circular SRR is 3.31 GHz while square SRR resonates at 2.67 GHz. Linear relationship is found between resonance shift and dielectric constant for both proposed sensors. Good coefficient of determination is obtained and the linear equation is used to predict the dielectric constant of Rogers RT6002, FR4 and Rogers TMM10 for validation purpose. Experiment measurement proved that the proposed circular and square SRR sensors have high accuracy in dielectric constant measurement.

ACKNOWLEDGEMENT

I would like to acknowledge and express my sincerest thanks to my supervisor, Ir Dr. Yeap Kim Ho for the continuous support and encouragement of my study and research. His patience, generous advice and guidance helped me throughout the research. It is a great pleasure to work under his supervision.

I thank my co-supervisor, Ir Dr. Teh Peh Chiong, for his kind help and support during the research.

My sincere thanks also go to the UTAR laboratory staff, Mr. Thong Marn Foo and Ms. Norazuani for their help in the fabrication and laboratory work.

Last but not least, I would like to thank my beloved family for their endless moral and physical support during my study.

APPROVAL SHEET

This dissertation/thesis entitled "**DESIGN AND DEVELOPMENT OF SPLIT-RING RESONATOR-BASED SENSORS FOR DIELECTRIC CONSTANT MEASUREMENT**" was prepared by OH ZI XIN and submitted as partial fulfillment of the requirements for the degree of Master of Engineering Science at Universiti Tunku Abdul Rahman.

Approved by:

(Ir. Dr. YEAP KIM HO)
Date: 22nd November, 2022
Supervisor
Department of Electronic Engineering
Faculty of Engineering and Green Technology
Universiti Tunku Abdul Rahman

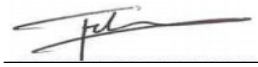

(Ir. Dr. Teh Peh Chiong)
Date: 22nd November, 2022
Co-supervisor
Department of Electronic Engineering
Faculty of Engineering and Green Technology
Universiti Tunku Abdul Rahman

FACULTY OF ENGINEERING AND GREEN TECHNOLOGY

UNIVERSITI TUNKU ABDUL RAHMAN

Date: 22nd November, 2022

SUBMISSION OF FINAL YEAR PROJECT /DISSERTATION/THESIS

It is hereby certified that ***OH ZI XIN*** (ID No: ***18AGM07420***) has completed this dissertation entitled "*Design and Development of Split-Ring Resonator-Based Sensors for Dielectric Constant Measurement*" under the supervision of Ir Dr. Yeap Kim Ho (Supervisor) from the Department of Electronic Engineering, Faculty of Engineering and Green Technology , and Ir Dr. Teh Peh Chiong (Co-Supervisor) from the Department of Electronic Engineering, Faculty of Engineering and Green Technology.

I understand that University will upload softcopy of my dissertation in pdf format into UTAR Institutional Repository, which may be made accessible to UTAR community and public.

Yours truly,

_____

(*Oh Zi Xin*)

DECLARATION

I hereby declare that the dissertation is based on my original work except for quotations and citations which have been duly acknowledged. I also declare that it has not been previously or concurrently submitted for any other degree at UTAR or other institutions.

Name OH ZI XIN

Date 22nd November, 2022

TABLE OF CONTENTS

LIST OF TABLES

LIST OF FIGURES

LIST OF ABBREVIATIONS

CPW	Coplanar Waveguide
CSRR	Complementary Split Ring Resonator
CTSRRs	Complementary Triangular Split Ring Resonators
GHz	Gigahertz
HFSS	High Frequency Structure Simulator
MHz	Megahertz
MUT	Material Under Test
SIW	Substrate Integrated Waveguide
SMA	SubMiniature version A
SRR	Split Ring Resonator
VNA	Vector Network Analyzer

LIST OF SYMBOLS

C_0	Total capacitance of circular SRR
C_{gap}	Capacitance of the slot ring of square SRR
C_m	Capacitance between square ring
C_{pul}	per-unit-length capacitance of circular SRR
C_s	Resultant capacitance of circular SRR
L_m	Inductance of square ring
L_s	Self-inductance of circular SRR
R^2	Coefficient of determination
f_r	Resonance frequency
r_0	Average radius of the circular rings
ε	Permittivity of substrate
ε_0	Permittivity of free space
ε_r	Relative permittivity
μ_0	Permeability of vacuum
Δf	Resonance frequency shift
D	Gap of the square ring
S	Space between the rings of square SRR
W	Width of the square ring
c	Width of the circular ring
g	Gap between the ring split
l	Length of the circular ring
t	Metal thickness of the circular ring

CHAPTER 1

INTRODUCTION

1.1 Research Background

Dielectric materials have poor electrical conductivity but they are polarizable (Martinez-Vega, 2013). The electrical properties of these substances are explained by the dielectric constant, $\varepsilon_r$which is defined as the ratio of the permittivity of the substance to the permittivity of the free space (Nelson, 2015). This parameter is important as the refractive indices and the capacitance of electronic devices are correlated to it (Luszczynska *et al*., 2019). Besides, it is also related to the material characteristics like water content, bulk density, biobased content, chemical absorption and the relationship between stress and strain. The widespread usage of dielectric constant is presented in food, medicine, electronic, construction, biology and agriculture industries (Büyüköztürk *et al*., 2006). Therefore, the measurement of dielectric constant becomes significant (Wang *et al*., 2021).

One of the common methods used for dielectric constant measurement is the transmission line measurement method (Li, 2017). The transmission line method requires the test sample to fit firmly with the transmission line (Szostak and Słobodzian, 2018; Sato *et al*, 2021). The next measurement method is the open-ended coaxial probe measurement. This method measures the reflection

coefficient by pressing the sensor onto the solid sample or immersing the sensor into the liquid sample (Lee *et al*., 2014). The coaxial probe measurement is commonly used in dielectric constant measurement due to its simple practicality and non-destructive properties (Fontana, Canicattì and Monorchio, 2019). Besides, the free space measurement method is suitable for the millimeter-wave range measurement (Liu *et al*., 2021) while the resonant cavity method has high precision in dielectric constant measurements (Jha and Akhtar, 2014).

In recent years, split-ring resonator (SRR) and its complementary (CSRR) gain high interest in microwave sensor design. The reason behind this is due to the good electrical properties, low profile, low radiative losses and high-quality factor of the resonance frequency band (Puentes *et al*., 2011; Oliveira *et al*., 2020). SRR topology consists of two concentric rings with a split faced opposite each other (Naqui, 2011). The inductance and capacitance within the SRR enable it to behave as an *LC* resonator.

Figure 1.1. Circular split-ring resonator

Inspired by previous works, circular and square SRR-based microwave sensors are developed here for dielectric constant measurement. Both sensors

are capable of measuring dielectric constants ε_r from 1.5 to 10.2. The resonance frequency of the SRR shifts when the material under test (MUT) is applied to the SRR sensors. The relationship between the resonance frequency shift and the dielectric constant can be used to predict the ε_r of unknown materials within the testing range.

1.2 Problem Statement

The dielectric constant is important in defining a substance's ability to store energy in an electric field (Nelson, 2015). However, the determination of dielectric constant requires high expenses, complex design and difficult sample preparation. The common methods used in dielectric measurement such as the transmission line measurement method, open-ended coaxial probe measurement, free space method and resonant cavity measurement have their strength and weakness (Venkatesh and Raghavan, 2005).

The transmission line method and resonant method have high accuracy in dielectric constant measurement but the sample preparation is quite difficult (Fontana, Canicattì and Monorchio, 2019). Besides, the open-ended coaxial probe method is suitable for high permittivity samples only (Lee *et al*., 2014) while the free space method is applicable for medium and high loss materials (Liu *et al*., 2021).

Hence, this study focuses on the microwave sensors design with the advantages of low-cost, small footprint and high accuracy.

1.3 Objective

This research aims to develop SRR-based microwave sensors with low-cost, simple measuring procedures, small in size and good performance advantages for dielectric constant measurement. Circular and square SRR-based sensors are designed in this research project.

The next objective is to analyze the relationship between the resonance frequency shift Δf and the dielectric constant ε_r of materials. The relationship is used to determine the dielectric constant of unknown materials.

The third objective is to validate the performance of the sensors by experimental measurement using a vector network analyzer (VNA). The comparison of the simulation results, experiment results and the standard values of the dielectric constant is the way to prove the sensor's performance.

1.4 Overview of Thesis

This thesis is to develop SRR-based microwave sensors with low-cost, small footprints and high accuracy for dielectric constant measurement. The thesis organization is as below:

Chapter 2 presents the literature review on the dielectric constant, measurement method and SRR implementation. Furthermore, the pros and cons of the previously proposed methods are discussed in this chapter.

Chapter 3 explains the methodology used in this research project. The design process, sensor simulation and experiment measurement for both circular and square SRR-based sensors are recorded.

Chapter 4 shows the analysis of the results. The relationship between the resonance frequency shift and dielectric constant is discussed and the performance of sensors is validated in this chapter.

Chapter 5 concludes with the findings of previous chapters. Besides, some of the future work is discussed in this chapter.

CHAPTER 2

LITERATURE REVIEW

This chapter gathers the literature and information regarding the dielectric constant measurement and the SRR implementation. The outcome of previous studies is significant for researchers to identify the existing problems and to develop method for improvement.

2.1 Introduction

The dielectric constant, also known as the relative permittivity. It explains the capability of a substance to store an electric field that is applied to it (Evans *et al*., 2007). This parameter is significant in physical and biological applications since it is related to the characteristics of the materials such as the water content, bio-content, chemical concentration and bulk density (Büyüköztürk *et al*., 2006). The dielectric constant ε_r can be defined as

$$\varepsilon_r = \frac{\varepsilon}{\varepsilon_0}$$

where

ε_r= relative permittivity

ε = permittivity of substance

ε_0= permittivity of free space

The ε_r is important in circuit and antenna designs as it can be used to correlate the dimension and performance of the antenna. According to Geambasu *et al.* (2014), a compact antenna can be developed by a high-dielectric material. The designed antenna has a compact size, low loss and good thermal stability.

Moreover, a high dielectric constant material is required for high energy density capacitor (Wang and Dang, 2018). This is because the capacitance of a capacitor is related to the dielectric constant. Chang *et al.* (2010) synthesized a high dielectric constant material for capacitor fabrication and explained the method used to increase the material's dielectric constant.

The dielectric constant ε_r can be applied in moisture content measurement. As the ε_r decreases along with the increase of moisture, the measurement of dielectric properties has been proposed to determine the moisture content in shelled peanuts by Trabelsi and Nelson (2008).

Besides, dielectric constant ε_r has also been widely used in the food industry. In the investigation performed by Shin *et al.* (2018), dielectric properties are important to maintain food quality and safety. Shin and his colleagues have used the dielectric traces to distinguish different types of food and insect samples.

The dielectric constant ε_r is correlated to blood glucose as well. The correlation between the blood glucose and the dielectric constant ε_r can be used to predict the blood glucose level (Park *et al*., 2003). The dielectric constant increases when the glucose level decreases. Besides, according to the recent research conducted by Zeng *et al*. (2018), the relation between the ε_r and blood glucose concentration made non-invasive blood glucose monitoring possible.

2.2 Dielectric Constant Measurement Methods

Various methods have been developed to measure dielectric constants. A review in the literature shows that the transmission/reflection line measurement, open-ended coaxial probe, free space method, and resonant cavity methods are among some of the popular ones employed for dielectric constant measurements. A brief illustration on these methods and their pros and cons are summarized here.

2.2.1 Transmission/Reflection Line Method

Measurements using the transmission line method require a sample to be placed inside a transmission line. This method measures both the reflection and transmission coefficient. Liu *et al*. (2019) proposed a transmission line method to measure 3D-printing materials. The material under test (MUT) is placed into a rectangular waveguide and the two-port S parameter is measured. However, the measurement results is susceptible to the air gap effects. This is

to say that the gap between the waveguide and the MUT has to be minimized in order to obtain accurate results.

A new planar transmission line method is presented by Bulja *et al.* (2009) for the dielectric measurement of liquid crystals. The liquid crystal cell is sandwiched between the strips of two microstrip lines. The researchers showed that the method was accurate in measuring MUTs operating from 57 GHz to 62 GHz. The method, however, suffers from difficulty in separating the sample cells.

Szostak and Słobodzian (2018) employed the two-port transmission/reflection line measurement to measure dielectric constants. It uses an adjustable width line to make self-calibration and improve impedance mismatch. However, the step discontinuity of connectors of the transmission line affects the accuracy of measurement.

2.2.2 Open-Ended Coaxial Probe Method

The open-ended coaxial probe method measures the dielectric constant based on the reflection coefficient amplitude and phase. (Venkatesh and Raghavan, 2005). The probe is pressed onto a solid sample or immersed in a liquid sample during the measurement.

Lee *et al.* (2014) proposed a dual open-ended coaxial sensor system to measure the dielectric constant. This method determines the dielectric constant

by using two magnitude measurements and has the advantages of low cost and simple measuring devices. Nevertheless, the dual open-ended coaxial method is suitable for samples with high permittivities only.

Dielectric constant measurement based on the coaxial probe method has the potential for biological sensing applications (Nakamura *et al*., 2020). Two layers of materials are measured using two coaxial probe sensors with different penetration depths. This method is independent of the measuring sample thickness but there is an inverse problem with the admittance model. The measurement accuracy is affected by the fringing field which is not stated in the proposed admittance model.

Moreover, Michiyama *et al.* (2006) proposed an obliquely cut open-ended coaxial probe for dielectric measurement of lossy material. The results prove that the proposed method is able to measure the deep point of a material. However, this measurement is suitable for materials operating within the low-frequency range only.

2.2.3 Free Space Method

The free space method usually includes two antennas that are opposite to each other and connected to a vector network analyzer (VNA) (Yaw, 2012).

The free space method is suitable for millimeter-wave measurements. Guo *et al.* (2020) have used the free space method to determine the dielectric

constant of liquid crystals in the millimeter-wave range. Calibration is required for this proposed method to enhance the performance of the measurement.

Besides, the free space method requires a large sample size for measurements. An improved free space technique was proposed by Pieraccini *et al*. (2018) to measure the dielectric properties of sawdust. The size of the material used in the measurement was 60 cm x 60 cm.

Yamaguchi and Sato (2017) used a monostatic horn antenna to improve the free space measurement. The proposed method was able to improve the complex dielectric constant measurements. In loss tangent measurements, however, the developed method is limited to lossy materials only.

2.2.4 Resonant Method

The resonant method has high accuracy in permittivity and permeability measurements. The resonance frequency and the quality factor of an empty resonant cavity are measured and followed by the measurement of a filled cavity. The dielectric constant is then computed using the frequency and quality factor by a numerical model.

A generalized two-step resonant cavity method was proposed by Jha and Akhtar (2014) to measure dielectric constants and loss tangents. The improved method has higher measurement sensitivity. Similarly, a generalized substrate integrated waveguide (SIW) cavity technique was proposed for permittivity

measurement by Tiwari *et al*. (2018). The proposed technique is, however, restricted solely to medium-loss dielectric substrates.

It is to be noted that, the resonant cavity measurement requires the sample to be filled inside the cavity. A modified cavity perturbation method was used to reduce the measurement error of a partially filled sample by Li and Li (2012). The improved formula reduces the error to 7% when the volume of the sample is above 50%.

2.3 Split-Ring Resonator (SRR)

Metamaterial is an artificial material engineered to have specific properties that are not usually found in nature (Chowdhury and Eroglu, 2020). The split-ring resonator (SRR) structure is capable of exhibiting the characteristics of metamaterials (Singh *et al*., 2021). As shown in Figure 2.1, the SRR and its complementary counterpart CSRR have similar topology -- viz they consist of two concentric rings with slits at opposite ends. The splits of the SRR increase the electrical energy and the loops of the SRR store the magnetic energy (Singh *et al*., 2021). The capacitance and inductance of the SRR structures make it to operate as an *LC* resonance circuit.

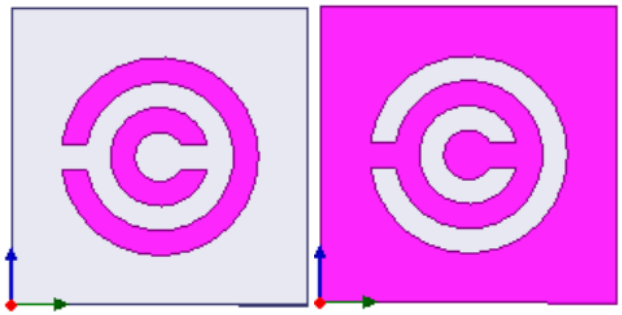

(a) (b)

Figure 2.1. Topology of (a) SRR and (b) CSRR

The SRR and CSRR have been widely embedded into antenna designs and microwave sensors because of the benefits of low cost, small footprint and good electrical properties (Oliveira *et al*., 2020).

Choudhary *et al.* (2021) implemented CSRR and rectangular slots in microstrip patch antenna to improve the antenna gain, size and directivity. The CSRR is placed on the radiating patch for dual-band response and gain enhancement.

Besides, the SRR is implemented to improve the antenna's radiation performance. Based the research performed by Kose and Kavas (2020), an SRR based antenna has higher gain and bandwidth compared to a conventional microstrip patch antenna.

Chatterjee and Kumar (2020) proposed a miniature elliptical waveguide using a square SRR. The SRR increases the electrical and magnetic energy of

the proposed waveguide and therefore reduces the dimension of the proposed waveguide. Besides, the SRR creates a passband in the cut-off region.

Furthermore, the application of SRRs can be found in filter designs. The complementary triangular split ring resonators (CTSRRs) was integrated into a patch antenna to develop a band-stop filter by Chandra (2021).

2.3.1 Dielectric Measurement by SRR-based Sensor

A dual-band SRR-based sensor was proposed for the dielectric measurement of milk (Del Carpio-Concha *et al*., 2021). The proposed SRR sensor has higher sensitivity and better resonance. The dielectric constant can be determined by a numerical model based on the resonance frequency shift. However, the proposed sensor was designed for liquid sample measurements only.

Moreover, a microstrip ring resonator is presented for dielectric constant extraction (Mahjabeen *et al*., 2020). The simulation and measurement results have a good agreement up to 8.5 GHz.

Other than that, the CSRR also show good performance in dielectric constant measurement. A dual split ring resonator-based sensor was proposed to measure the dielectric constant of the testing sample (Shahzad *et al*., 2020). The CSRR is integrated in the ground plane of the sensor and loaded with a microstrip line. Dielectric constants can be calculated based on the resonance

frequency and magnitude of the CSRR sensor. It is to be noted that, there are only three samples were used in the measurements.

In Chuma *et al*. (2018), the CSRR sensor was used as a sensor to determine both the permittivity and the loss tangent of materials at 22 GHz. The shift of the resonance frequency is correlated to the dielectric constant of the MUT while the resonant magnitude is dependent on the loss tangent of the materials. The proposed method is non-destructive, economical and has high accuracy. It is proved by the close agreement between the measurement results and the standard values stated in the datasheet. However, some materials may not be suitable to be measured at this high-frequency range, which is 22 GHz.

By characterizing the interrelation between the resonance frequency displacement and dielectric constant, the dielectric properties of materials can be determined by an SRR-based microwave sensor.

In order to improve the performance of the dielectric measurement sensors for dielectric constant measurement, a circular and a square SRR-based sensor are proposed in this work. The designed sensors should have a wide measuring range, which involves more testing samples in the measurement. Besides, the measurement setup of the proposed sensors should be simple and the operating frequency is appropriate for the material under test (MUT).

2.4 Summary

In summary, the dielectric constant plays an important role in diverse areas. The methods proposed previously including the transmission line measurement method, open-ended coaxial probe measurement, free space measurement and resonant cavity method have their own advantages and limitations. The transmission line and the resonant cavity method require the testing sample to fit with the coaxial line or resonant cavity. The accuracy of the open-ended coaxial probe method is dependent on the air gap effect while the free space method requires a large sample size and has limited bandwidth. Recently, the SRR technique has been widely used in microwave sensor design. The good electrical properties of SRRs make them suitable for various parameter measurements, including the dielectric constant.

CHAPTER 3

METHODOLOGY

This chapter presents the design configurations of the circular and square SRR-based sensors, the simulation procedure and the experimental measurements. The sensors' designs are based on an SRR coupled with a coplanar waveguide (CPW) transmission line. The theoretical formulations, sensors' simulations and measurement methods are explained here.

3.1 Introduction

Two types of SRR-based sensors are proposed for the dielectric constant measurement, one is a circular SRR-based sensor while the other is a square SRR-based sensor. The dimensions of the SRRs are calculated based on the equations in Baena *et al*. (2005) and Naoui *et al*. (2016) and the designs are then simulated by Ansys High-Frequency Structure Simulator (HFSS) to get the preliminary results. The finalized designs are fabricated on a Rogers RO3210 substrate and the experimental measurements are carried out using a vector network analyzer (VNA) for validation purposes. The transmission coefficient, S21 parameter for the unloaded sensor and the sensor with different materials under test (MUTs) applied onto it are recorded. Besides, the measurement results of this work are benchmarked with the open-ended coaxial probe method proposed by Lee *et al*. (2014). The coaxial probe method has been chosen in

this case since it provides sufficiently good accuracy and the measurement setup is comparatively simple.

3.2 Sensors Design

Both the circular and square SRR-based sensors consist of an SRR printed on the top of the substrate and coupled with a CPW transmission line at the bottom. The sensors' resonance frequency depends on the substrate's relative permittivity, substrate thickness and the dimensions of the SRR ring. Both sensors are printed on a Rogers RO3210 substrate, with a relative permittivity of 10.2, loss tangent of 0.003 and thickness of 1.27 mm.

3.2.1 Circular SRR-based Microwave Sensor

Figure 3.1 shows the design configuration and geometrical parameters of the circular SRR sensor.

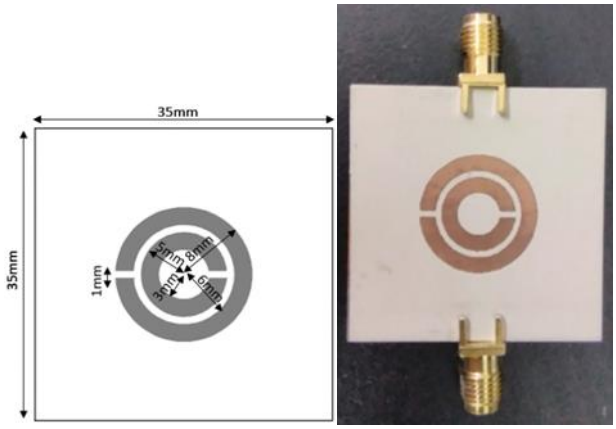

(a)

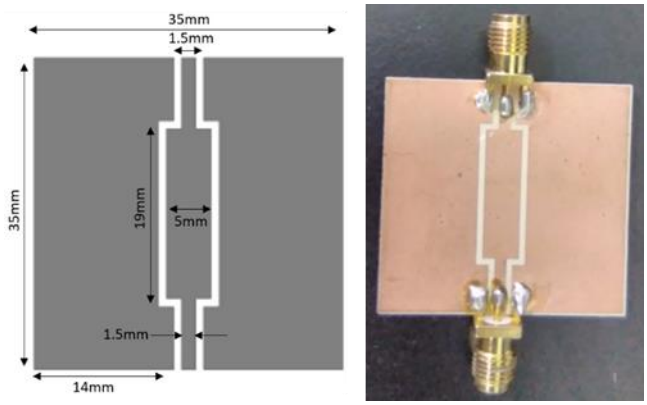

(b)

Figure 3.1. The (a) top and (b) bottom configurations of the proposed circular SRR-based sensor

The circular SRR has an LC equivalent circuit as presented in Figure 3.2 (Baena *et al*., 2005). The SRR behave like an *LC* circuit.

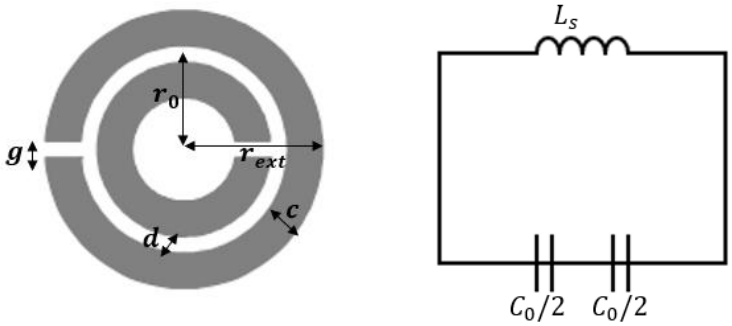

Figure 3.2. Equivalent circuit of a circular SRR

The L_s in Figure 3.2 denotes the self-inductance of the SRR structure, C_0 defines the total capacitance between the rings, $C_0 = 2\pi r_0 C_{pul}$, where r_0 is the average radius of the rings and C_{pul} is the per-unit-length capacitance. C_s, the resultant capacitance is given by $C_s = C_0/4$.

The resonance frequency of a circular SRR is predicted from the formula $f_r = \frac{1}{2\pi\sqrt{L_s C_s}}$, the L_s and C_s are obtained by the formula,

$$L_s = 0.002l \log\left(\frac{4l}{c} - \gamma\right) \mu H \quad (1)$$

$$C_s = \frac{\varepsilon_0 ct}{2g} + (\pi r_0 - g)\left(\frac{C_{pul}}{2}\right) \text{ F} \quad (2)$$

where, l is the length of the ring, $\varepsilon_0$is the absolute permittivity, c is the width of the ring, t is the metal thickness and g is the gap between the split.

3.2.2 Square SRR-based Microwave Sensor

The structure design of the square SRR-based microwave sensor are shown in Figure 3.3. Similarly, the resonance frequency of the square SRR sensor is determined by the formula $f_r = \frac{1}{2\pi\sqrt{L_m(C_m + C_{gap})}} \approx f_r = \frac{1}{2\pi\sqrt{L_m C_m}}$ (Naoui *et al*., 2016).

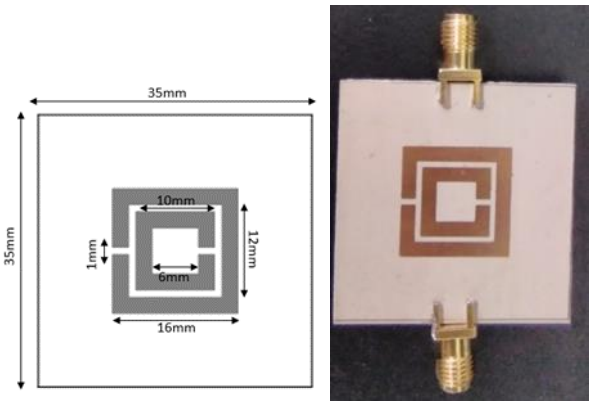

(a)

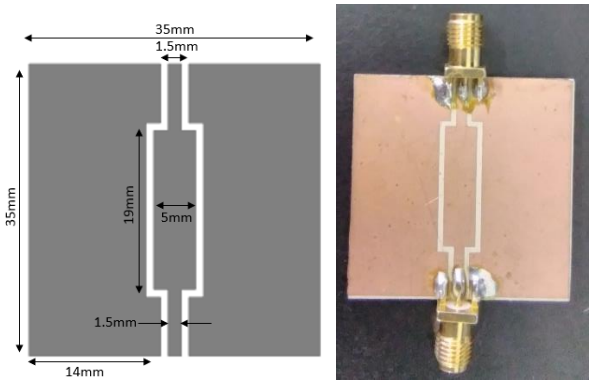

(b)

Figure 3.3. The (a) top and (b) bottom configurations of the proposed square SRR-based sensor

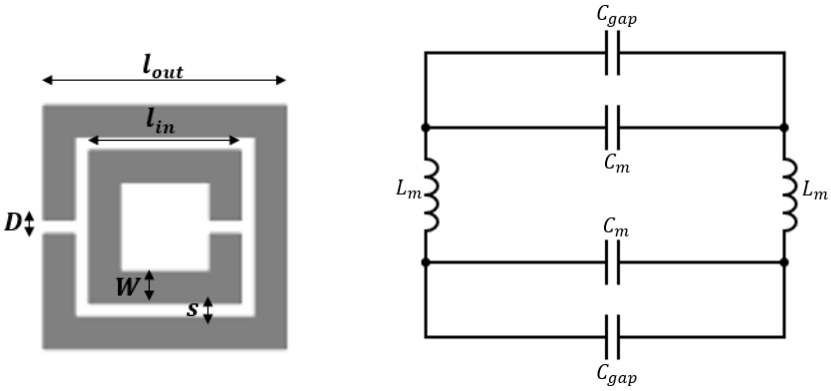

Figure 3.4. Equivalent circuit of a square SRR

The L_m, C_{gap} and C_m can be determined by the equations,

$$L_m = \frac{\mu_0 S}{W}[l_{out} + l_{in}] \quad (3)$$

$$C_{gap} = \frac{\varepsilon_0 \varepsilon_r t_c}{D} \quad (4)$$

$$C_m = \frac{A\varepsilon_0 \varepsilon_r W(2l_{out}+2l_{in}-D)}{2S} \quad (5)$$

where, μ_0 is the permeability of vacuum, S is the space between rings, W is the width of the ring and D is the gap of ring.

3.3 Simulation of Proposed Sensors

The proposed circular and square SRR-based sensors are simulated by Ansys HFSS, a 3D electromagnetic simulation software used to design, develop and simulate the high-frequency electronic components including antennas, microwave components and sensors.

A Rogers RO3210 substrate with a size of 35 mm x 35 mm x 1.27 mm is drawn on the HFSS 3D modeler window. The SRR is drawn on the top of the substrate while the CPW transmission line is at the substrate's bottom. For the circular SRR sensor, the two concentric circular rings have a mean radius of 5.5 mm. The square SRR, on the other hand, has an outer length of 16 mm and an inner length of 10 mm.

Both ends of the proposed SRR-based sensors are connected to a pair of wave ports. The wave ports are used to excite the electromagnetic waves into the transmission line. The radiation boundary is set in the simulation to create an open model. The next step is to add an analysis setup and to run the simulation. Figure 3.5 shows the Ansys HFSS design layout for both sensors.

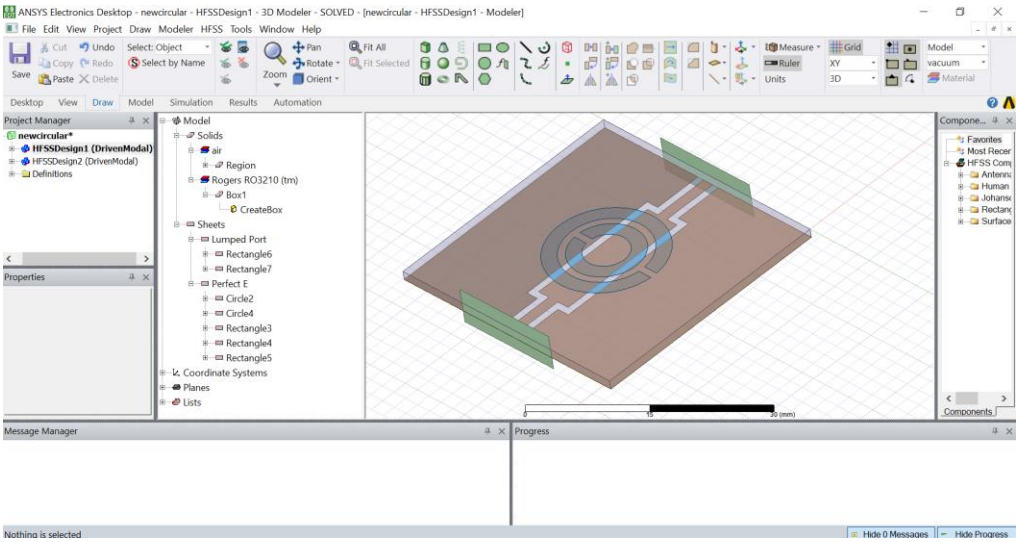

(a)

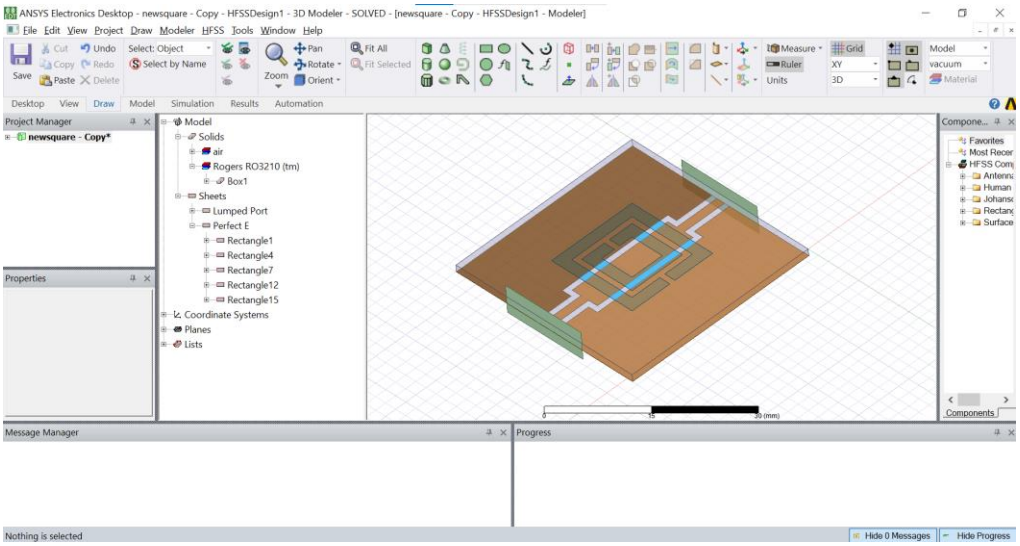

(b)

Figure 3.5. HFSS design (a) circular SRR-based sensor and (b) square SRR-based sensor

13 sets of materials with dielectric constant ε_r from 1.5 to 10.2 are selected to correlate the dielectric constant ε_r with the resonance frequency shift Δf. As shown in Figure 3.6, the sample is drawn on the top of SRR. The permittivities of the samples are set according to their standard dielectric

constant values which are stated in Table 3.1. The resonance frequency shift for each sample is recorded and discussed in the next chapter.

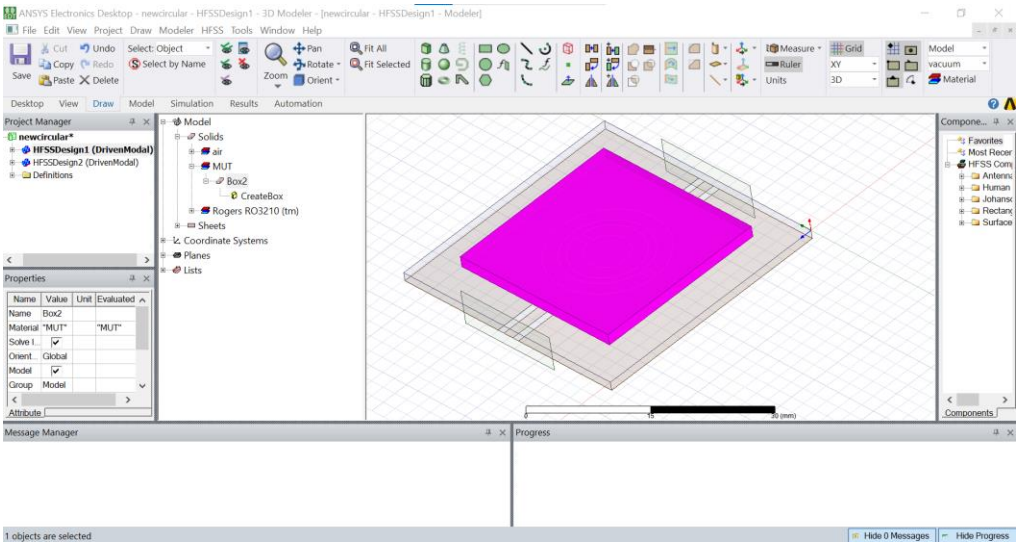

Figure 3.6. MUT applied to the proposed sensor

Table 3.1. Materials used in measurement

Material	Standard Dielectric Constant
Resin	1.5
Sugar	2
Rogers RT5880	2.2
Clay	2.3
Rubber	2.9
Rice	3
Oakwood	3.3
Quartz	4.3
Porcelain	5.7
Mica	6

Neoprene	7.5
Glass	9.15
Rogers RO3210	10.2

3.4 Experiment Measurement

The design layout of both sensors is exported from the HFSS software and fabricated on a Rogers RO3210 substrate. The both ends of the CPW transmission line are connected to a pair of SMA connectors. The SMA connectors are then connected to a vector network analyzer (VNA) for measurement.

As shown in Figure 3.7, the SRR-based sensor is connected to the VNA and the two port S-parameter measurement is carried out. The transmission coefficient, S21 resonance frequency of the unloaded sensor is measured and recorded as the reference frequency. Figure 3.8 illustrates the experimental setup for the sample measurement. Each sample is loaded onto the SRR structure and its resonance frequency shift is observed. The relationship between the resonance frequency shift and dielectric constant is correlated graphically. By formulating an equation to describe the graph, the dielectric constant of an unknown material can therefore be easily determined.

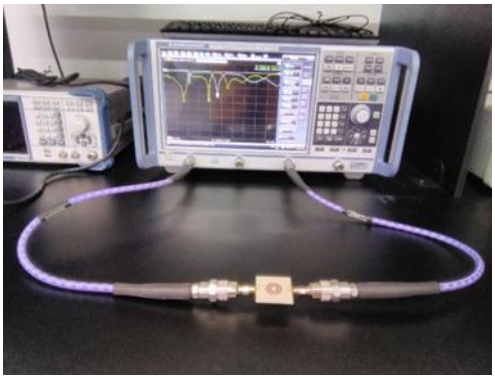

Figure 3.7. Experiment setup for measurement (unloaded sensor)

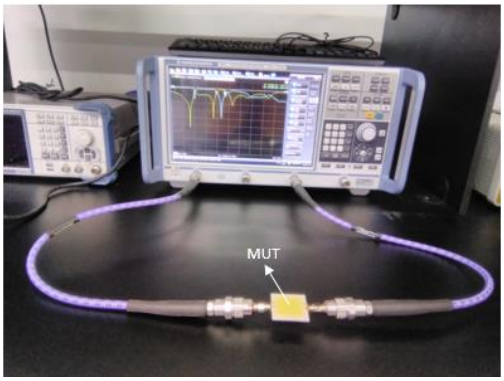

Figure 3.8. Resonance shift measurement when MUT is applied

In order to validate the accuracy of the equation, three substrate materials, i.e., Rogers RT6002, FR4 and Rogers TMM10 with relative permittivities of 2.94, 4.4 and 9.2 respectively are used. The measurement results are compared to the standard values stated in the datasheet.

The results obtained from the experimental measurement are also benchmarked with the values obtained by the open-ended coaxial probe method proposed by Lee *et al.* (2014). In the coaxial probe method, a modified SMA connector as shown in Figure 3.9 is used as the probe sensor. The SMA stub is pressed against the sample to measure the reflection coefficient in the form of

magnitude and phase. Figure 3.10 shows the experiment measurement setup of the open-ended coaxial probe method. The reflection coefficient is measured by a VNA and the dielectric constant is determined by a numerical model.

Figure 3.9. SMA stub used as the open-ended coaxial probe sensor

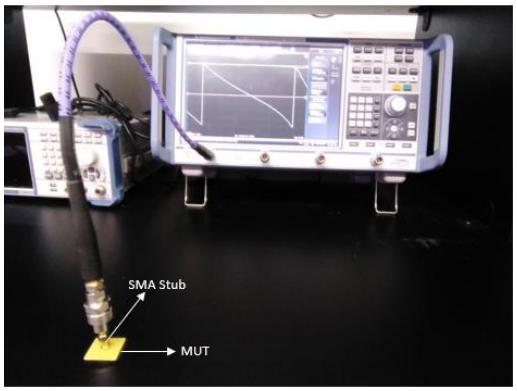

Figure 3.10. Measurement setup of coaxial probe method

3.5 Summary

In this chapter, the simulation and experiment procedures are discussed. The proposed microwave sensors are first simulated using Ansys HFSS and they are then fabricated for validation. The sensor's resonance frequency is measured using a vector network analyzer (VNA). There are 13 samples with the standard dielectric constant ε_r ranging from 1.5 to 10.2 used in the dielectric measurement. The resonance frequency shift is correlated with the dielectric

constant and the defined equation is able to predict the ε_r of the material under test (MUT). The measurement result is compared with the coaxial probe method proposed by Lee *et al*. (2014).

CHAPTER 4

RESULTS AND DISCUSSION

In this chapter, the results of the simulation and the measurement are analyzed and discussed. The relationship between the resonance frequency shift Δf and the dielectric constant ε_r is correlated graphically. By applying an equation to explain the graph, the dielectric constant of an unknown material can be determined easily. The results analysis and discussion are presented in the following section.

4.1 Introduction

There are 13 sets of materials with the ε_r ranging from 1.5 to 10.2 used in this work to correlate the resonance shift to the dielectric constant. The resonance frequency is found to red shift towards a lower value when the dielectric constant of materials increases. The measurement results agree closely with the simulation results and the standard dielectric constant indicated in the datasheet.

4.2 Circular SRR-based Sensor Results

In the measurement, the MUT is deposited at the center of the sensor. The unloaded circular SRR sensor has a resonance frequency of 3.31 GHz. As

presented in Figure 4.1, the resonance frequency of the transmission coefficient shifts towards a lower value when MUT is applied. This is because the capacitance of the SRR structure is affected by the increasing permittivity of its surroundings.

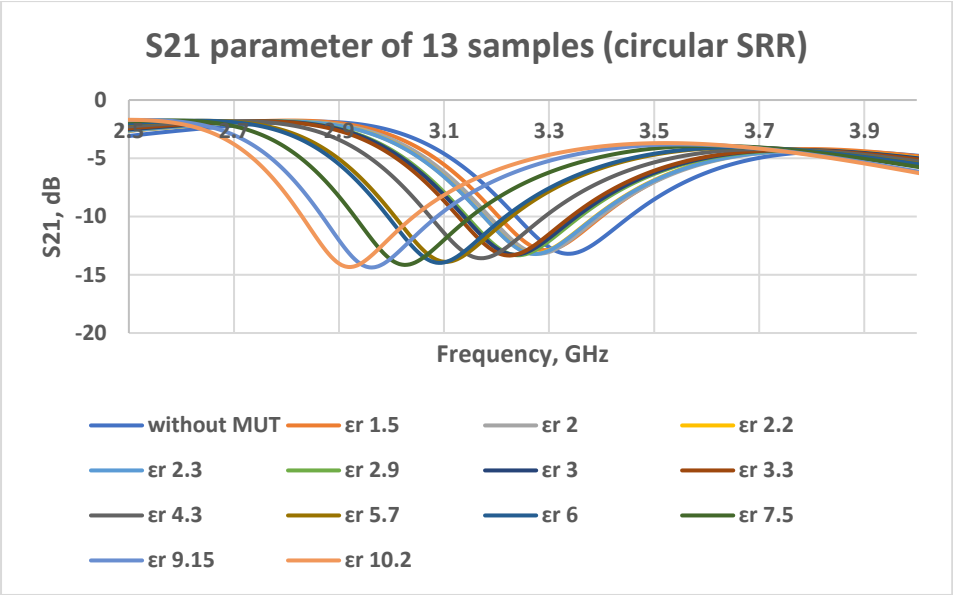

Figure 4.1. Resonance shifts for different dielectric constant (circular SRR)

Figure 4.2 presents the correlation between the resonance frequency shift Δf and the dielectric constant ε_r of material. The resonance frequency of the unloaded sensor is known as f_0, the resonance frequency at each dielectric constant ε_r is recorded as f_r, and the resonance shift Δf is calculated by $\Delta f = f_r - f_0$.

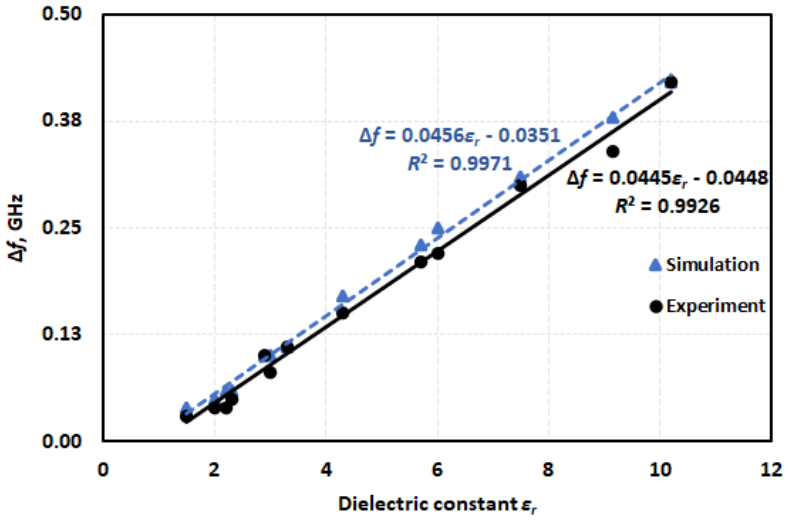

Figure 4.2. Resonance shift vs dielectric constant (circular SRR)

Both simulation results and experiment results show a linear relationship between the Δf and the ε_r. It can be seen that, the simulation and the measurement results agree strongly with each other. The linear equations obtained from the simulation and measurement results are expressed as $\Delta f = 0.0456\varepsilon_r - 0.0351$ and $\Delta f = 0.0445\varepsilon_r - 0.0448$ respectively. The equations allow the determination of dielectric constant within the range of 1.5 to 10.2.

The coefficient of determination R^2 is above 0.99 for both simulation and experiment measurement. R^2 is also known as the square of the correlation between the resonance shift Δf and the dielectric constant ε_r. It explains the proportion of variance in the resonance shift that is predictable by the material's dielectric constant (Turney, 2022). The high R^2 indicates that the simulation and measurement data fit the linear regression model well. The coefficient of determination R^2 is calculated by the equation,

$$R^2 = \frac{[n(\Sigma\varepsilon_r\Delta f)-(\Sigma\varepsilon_r)(\Sigma\Delta f)]^2}{[n\Sigma{\varepsilon_r}^2-(\Sigma\varepsilon_r)^2][n\Sigma(\Delta f)^2-(\Sigma\Delta f)^2]} \quad (6)$$

4.3 Square SRR-based Sensor Results

Figure 4.3 shows the resonance shift at the transmission coefficient of the square SRR sensor. The resonance frequency of the unloaded square SRR is 2.67 GHz and the resonance shifts to 2.37 GHz when the dielectric constant is increased to 10.2.

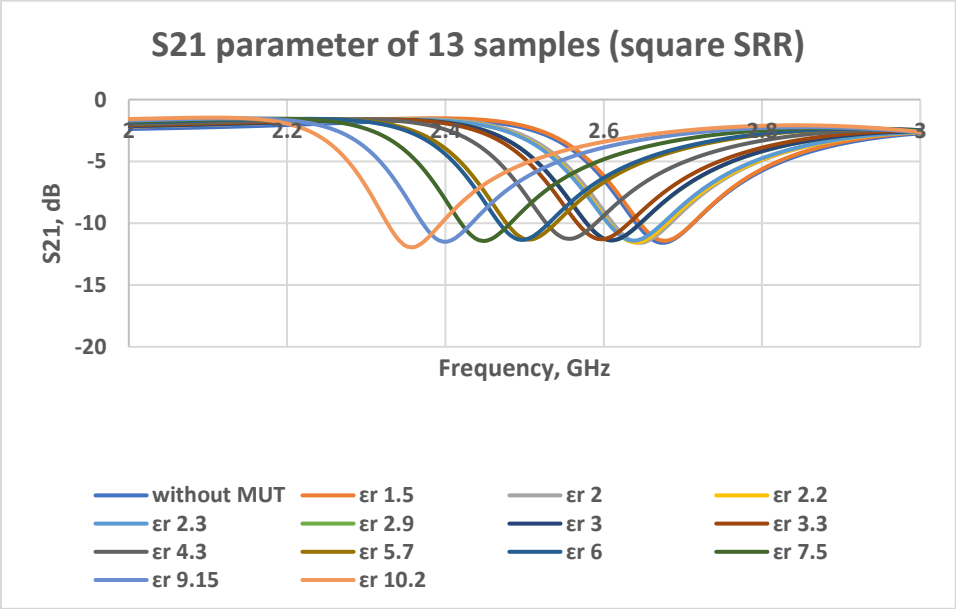

Figure 4.3. Resonance shifts for different dielectric constant (square SRR)

The resonance frequency is found to red shift towards a lower value when the dielectric constant increases. This is because the resonance frequency is inversely correlated to the capacitance.

The linear correlation between the resonance frequency shift Δf and the dielectric constant ε_r is described in Figure 4.4.

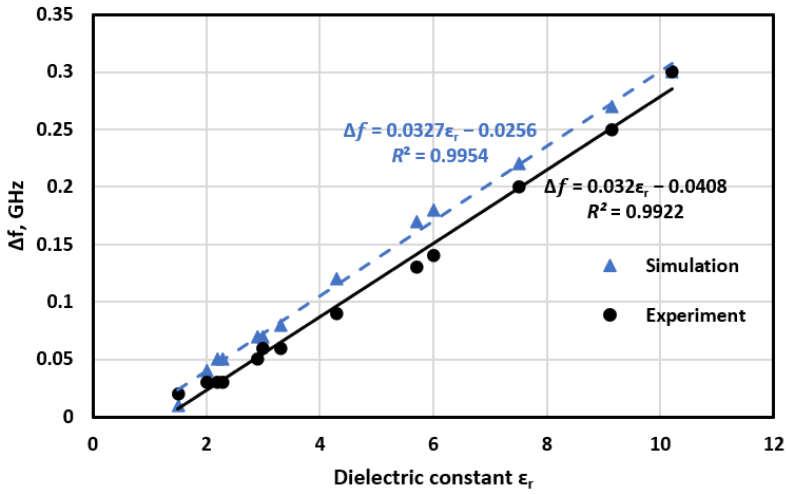

Figure 4.4. Resonance shift vs dielectric constant (square SRR)

As can be seen from the results, the simulation and experiment data fit the linear regression model well as the coefficient of determination R^2 is above 0.99. The slight differences found between the simulation and experiment data may due to the fabrication tolerance.

4.4 Validation of Sensors Performance

Three substrate materials, namely Rogers RT6002, FR4, and Rogers TMM10, are used to validate the performance of the sensors. The standard dielectric constant of the three substrate materials are 2.94, 4.4 and 9.2 respectively. By applying the inverse linear regression, the dielectric constant of the materials can be predicted by the equations,

$$\varepsilon_r = 22.47\Delta f + 1.007 \quad (7)$$

for circular SRR sensor and

$$\varepsilon_r = 31.25\Delta f + 1.275 \quad (8)$$

for square SRR sensor.

The measurement result from this work is then compared with the coaxial probe method proposed by Lee *et al*. (2014). The comparisons of both measurement results with the standard dielectric constant values are presented in Table 4.1.

Table 4.1. Comparison between the standard and measured dielectric constant

MUT	**Standard Dielectric Constant**	**Circular SRR**		**Square SRR**		**Coaxial Probe Method**	
		Dielectric Constant	**Difference with Standard Value (%)**	**Dielectric Constant**	**Difference with Standard Value (%)**	**Dielectric Constant**	**Difference with Standard Value (%)**
RT6002	2.94	2.80	4.76	2.84	3.40	2.61	11.22
FR4	4.40	4.38	0.45	4.40	0.00	4.28	2.73
TMM10	9.20	8.87	3.59	9.09	1.20	9.88	7.39

The results show that the inverse linear regression model can be used to predict the dielectric constant of an unknown material, as long as it lies within

the testing range 1.5 to 10.2. The proposed SRR sensors exhibit close agreement with the standard value given by datasheet, with discrepancy less than 4.76%, compared to the coaxial probe method, with discrepancy vary from 2.73% to 11.22%.

4.5 Comparison of Circular and Square SRR Sensors

Both sensors have a compact size of 35 mm x 35 mm x 1.27 mm and they are portable enough to be used with a nano-VNA. The circular and square SRR have different resonance frequencies although the SRR dimensions are similar. Based on the results, circular SRR has a higher resonance frequency (3.31 GHz) compared to square SRR (2.67 GHz). This result is in line with the previous research conducted by Saha and Siddiqui (2011).

The comparison between circular and square SRR sensors shows that the circular SRR has higher value of resonance shift compared to square SRR. The Δf of circular SRR is up to 420 MHz when the dielectric constant is increased to 10.2 while the highest Δf of square SRR is 300 MHz. The higher resonance shift indicates that the circular SRR-based sensor has better sensitivity compared to the square SRR-based sensor.

As explained in the previous section, both SRR sensors have the similar properties in dielectric constant measurement. The shift of the resonance frequency is related to the variation of the relative permittivity of MUT. Both circular and square SRR results obtained a high R^2 value for the linear

regression model and high accuracy in dielectric constant measurement, with error less than 4.76%.

4.6 Summary

The simulation result and the measurement result of the proposed SRR-based sensors show close agreement with each other. A linear relationship is obtained between the resonance frequency shift and the material's dielectric constant. In order to validate the sensors' performance and accuracy, three substrate materials with known relative permittivity are used as the test sample in the measurement. The comparison results proved that the proposed circular SRR-based sensor and square SRR-based sensor have high accuracy in determine dielectric constant within the testing range ε_r from 1.5 to 10.2, with error less than 4.76%.

CHAPTER 5

CONCLUSIONS AND RECOMMENDATIONS

In this chapter, the conclusions drawn from the findings of the development of split ring resonator-based sensors are presented. The conclusions are based on the research objectives, problem statement and the outcomes of the study. Besides, the recommendations are also described in the following section.

5.1 Research Overview

This research is carried out to design and develop split-ring resonator-based microwave sensors for dielectric constant measurement. Split-ring resonator (SRR) with good electrical properties and good sensitivity towards the surrounding permittivity is implemented in the proposed sensors.

There are two types of SRR sensors proposed in this work, which are circular and square SRR-based sensors. Both SRRs have a similar footprint and loaded a CPW transmission line. The proposed sensors are fabricated on the Rogers RO3210 substrate with a relative permittivity of 10.2 and a size of 35 mm x 35 mm x 1.27 mm. The material under test (MUT) is put on the SRR structure to determine the shift of the transmission coefficient resonance.

The correlation between the resonance frequency shift and dielectric constant can be explained by a linear regression model. The simulation and measurement results proved that the circular and square SRR sensors have high accuracy in dielectric constant measurements. The SRR-based sensors have the advantages of small footprint, high accuracy and non-destructive.

5.2 Summary of Results

The circular and square SRR designs are simulated by Ansys HFSS and they are then fabricated for validation. As shown by the results, the experimental measurements agree well with the simulation results. Both results exhibit a linear relationship between the resonance frequency shift and the dielectric constant, with R^2 above 0.99. The linear equation obtained from the measurement is applied to predict the dielectric constant ε_r of Rogers RT6002, FR4 and Rogers TMM10, with standard values of 2.94, 4.4 and 9.2 respectively.

For circular SRR measurements, the differences found between the measurement results and the standard dielectric constant for the three substrate materials are 4.76%, 0.45% and 3.59% respectively while the percentage error between the square SRR measurement and the referenced values are 3.40%, 0.00% and 1.20%.

In conclusion, the proposed SRR-based microwave sensors show high accuracy in measuring MUTs with dielectric constants from 1.5 to 10.2. This

research presents an alternative measurement method with the strength of small size, high sensitivity and simple measuring setup.

5.3 Recommendations

In this work, circular and square SRR-based microwave sensors are proposed to measure the dielectric constant of an unknown material. The working of the proposed sensors is based on the change of resonance frequency with respect to the variation of the dielectric constant ε_r of materials. After a thorough study, the recommendations for the future work are propose here.

Future studies should emphasize the impedance matching of the transmission line. The problem of the impedance mismatch may affect the performance of sensors. The efficiency of the SRR-based microwave sensors can be improved by a good return loss as more power can be delivered from the source to the load.

Besides, the measuring range of the proposed sensors can be increased to a higher value, which allows the sensors to measure MUTs with a higher dielectric constant.

The orientations of the SRR rings could be adjusted to optimize the performance of the SRR. Moreover, the different shapes of SRR structure can be implemented into the proposed microwave sensors. The comparison and analysis of the results of different type of SRRs may help to enhance the

measurement accuracy, sensitivity and the overall performance of the proposed sensors.

REFERENCES

Baena, J. D., Bonache, J., Martín, F., Sillero, R. M., Falcone, F., Lopetegi, T., Laso, M. A., Garcia-Garcia, J., Gil, I., Portillo, M. F., and Sorolla, M. (2005). Equivalent-circuit models for split-ring resonators and complementary split-ring resonators coupled to planar transmission lines. *IEEE transactions on microwave theory and techniques*, 53(4), 1451 – 1461.

Bulja, S., Mirshekar-Syahkal, D., Yazdanpanahi, M., James, R., Day, S. E., and Fernández, F. A. (2009). Planar transmission line method for measurement of dielectric constants of liquid crystals in 60 GHz band. *2009 Asia Pacific Microwave Conference*, Singapore, 341 – 344.

Büyüköztürk, O., Yu, T. Y., and Ortega, J. A. (2006). .: A methodology for determining complex permittivity of construction materials based on transmission-only coherent, wide-bandwidth free-space measurements. *Cement and Concrete Composites*, 28(4), 349 – 359.

Chandra, S. (2021). Dual Band Filtenna Design using Complementary Triangular Split Ring Resonators. *2021 Innovations in Power and Advanced Computing Technologies (i-PACT),* Kuala Lumpur, Malaysia, 1 – 5.

Chang, H. M., Wu, M. L., Chen, L. S., Huang, Y. J., and Fu, S. L. (2010). Study of high dielectric constant capacitors on flexible substrates. *2010 5th International Microsystems Packaging Assembly and Circuits Technology Conference,* Taipei, Taiwan, 1 – 4.

Chatterjee, S. and Kumar, S. S. (2020). Miniature Elliptical Waveguide Antenna Design Using Square Split Ring Resonator. *2020 URSI Regional Conference on Radio Science (URSI-RCRS),* Varanasi, India, 1 – 3.

Choudhary, A. K., Barman, S., Moyra, T., Debnath, A., and Bhattacharjee, A. (2021). Gain Enhancement of Dual-Band Microstrip - Fed Antenna with complementary split ring resonators and rectangular slots embedded in Patch for Wireless Applications using Metamaterial Cell-Based Superstrate. *2021 2nd International Conference on Range Technology (ICORT),* Chandipur, Balasore, India, 1 – 6.

Chowdhury, B. and Eroglu, A. (2020). Metamaterial Sensor Design With Split Ring Resonators. *2020 IEEE International Symposium on Antennas and Propagation and North American Radio Science Meeting,* Montreal, Canada, 733 – 734.

Chuma, E. L., Iano, Y., Bravo Roger, L. L., and Fontgalland, G. (2018). Using Metamaterial Complementary Split-Ring Resonators for Measuring Dielectric Constants and Loss Tangents at 22 GHz. *2018 3rd*

International Symposium on Instrumentation Systems, Circuits and Transducers (INSCIT), Bento Gonçalves, Brazil, 1 – 5.

Del Carpio-Concha, P., Nuñez-Flores, A., Acosta-Araníbar, R., and Castillo-Araníbar, P. (2021). Microwave Sensor Based on Split Ring Resonators for Dielectric Characterization of Density and Viscosity of Milk. *2020 IEEE MTT-S Latin America Microwave Conference (LAMC 2020),* Cali, Colombia, 1 – 4.

Evans, R., Frost, M., Stonecliffe-Jones, M., and Dixon, N. (2007). Assessment of In Situ Dielectric Constant of Pavement Materials. *Journal of the Transportation Research Board*, 2037, 128 – 135.

Fontana, N., Canicatti, E., and Monorchio, A. (2019). An application of the virtual transmission line model of an open-ended coaxial probe for dielectric properties characterization of biological tissues. *2019 IEEE International Symposium on Antennas and Propagation and USNC-URSI Radio Science Meeting,* Atlanta, USA, 341 – 342.

Geambasu, D. C., Leontin, T., Banciu, M. G., Nedelcu, L., and Nicolaescu, I. (2014). Compact antenna using ZST low-loss high dielectric constant material. *2014 22nd Telecommunications Forum Telfor (TELFOR),* Belgrade, Serbia, 807 – 809.

Guo, W., Xu, H., Liang, W., Liu, K., and Gao, Q. (2020). Free Space Method for Measurement of Millimeter-Wave Dielectric Properties of Liquid Crystals. *2020 Cross Strait Radio Science & Wireless Technology Conference (CSRSWTC),* Fuzhou, China, 1 – 3.

Jha, A. K. and Akhtar, M. J. (2014). A Generalized Rectangular Cavity Approach for Determination of Complex Permittivity of Materials. *IEEE Transactions on Instrumentation and Measurement*, 63(11), 2632 – 2641.

Kose, U. and Kavas, A. (2020). Design and Performance Analysis of Split Ring Resonator Based Microstrip Antenna With Defected Ground Structure. *2020 4th International Symposium on Multidisciplinary Studies and Innovative Technologies (ISMSIT),* Varanasi, India, 1 – 3.

Lee, K. Y., Chung, B. K., You, K. Y., Cheng, E. M., and Abbas, Z. (2014). Study of dual open ended coaxial sensor system for calculation of phase using two magnitudes. *IEEE Sensors Journal*, 14, 129 – 135.

Li, J. Y. (2017). Permittivity Measurement of Low-Loss Substrates Based on Split Ring Resonators. *World Journal of Engineering and Technology*, 5, 62 – 68.

Li, Z. and Li, E. (2012). Study on measurement of dielectric constant of partially filled material using modified cavity perturbation technique. *The 2012 International Workshop on Microwave and Millimeter Wave Circuits*

and System Technology, Chengdu, China, 1 – 3.

Liu, X., Gan, L., and Yang, B. (2021). Millimeter-wave free space dielectric characterization. *Measurement,* 179, 109472.

Liu, Y., Wan, H., Bao, Y., Xie, Y., and Zhang, Y. (2019). Dielectric Constant Measurement and Error Analysis of 3D-Printing Materials For Microwave Applications. *2019 International Applied Computational Electromagnetics Society Symposium - China (ACES),* Nanjing, China, 1 – 2.

Luszczynska, B., Matyjaszewski, K., and Ulanski, J. (2019). Photogeneration of Charge Carriers in Solution-Processable Organic Semiconductors. In: *Solution-Processable Components for Organic Electronic Devices*. John Wiley & Sons.

Mahjabeen, N., Bright, J., Aroor, S. R., Virushabadoss, N., Surendar, S., Elassy, K. S., Shiroma, W. A., Ohta, A. T., and Henderson, R. (2020). Low-Cost Rapid Prototyping of Ring Resonator for Dielectric Characterization of Packaging Substrates. *2020 IEEE Texas Symposium on Wireless and Microwave Circuits and Systems (WMCS),* Waco, TX, USA, 1 – 4.

Martinez-Vega, J. (2013). Physics of Dielectric. In: *Dielectric Materials for Electrical* Engineering. (pp. 1 – 16). John Wiley & Sons.

Michiyama, T., Tanabe, E., and Nikawa, Y. (2006). Obliquely cut open ended coaxial probe for obtaining complex permittivity of lossy materials. *2006 Asia-Pacific Microwave Conference,* Yokohama, Japan, 587 – 590.

Nakamura, M., Tajima, T., and Seyama, M. (2020). Two-Coaxial-Probe Method for Dielectric Spectroscopy of Two-Layer Materials Towards Biological Application. *2020 IEEE MTT-S International Microwave Biomedical Conference (IMBioC),* Toulouse, France, 1 – 3.

Naoui, S., Latrach, L., and Gharsallah, A. (2016). Equivalent circuit model of double split ring resonators. *International Journal of Microwave and Optical Technology,* 11(1), 1 – 6.

Naqui, J., Durán-Sindreu, M., and Martín, F. (2011). Novel sensors based on the symmetry properties of split ring resonators (SRRs). *Sensors,* 11(8), 7545 – 7553.

Nelson, S. O. (2015). Theory and Fundamental Principles. In: *Dielectric Properties of Agricultural Materials and their Applications*. (pp. 1 – 8). Athens, GA. Elsevier Inc.

Oliveira, J. G., Pinto, E. N., Silva Neto, V. P., and D'Assunção, A. G. (2020). CSRR-based microwave sensor for dielectric materials characterization

applied to soil water content determination. *Sensors,* 20(1:255).

Park, J. –H., Kim, C. –S., Choi, B. –C., and Ham, K. –Y. (2003). The correlation of the complex dielectric constant and blood glucose at low frequency. *Biosensors and Bioelectronics,* 19(4), 321 – 324.

Pieraccini, M., Miccinesi, L., and Rojhani, N. (2018). A Free-space Technique for Measuring the Complex Dielectric Constant of Sawdust. *2018 IEEE Conference on Antenna Measurements & Applications (CAMA),* Sweden, 1 – 3.

Puentes, M. Weiß, C., Schüßler, M., and Jakoby, R. (2011). Sensor array based on split ring resonators for analysis of organic tissues. *2011 IEEE MTT-S International Microwave Symposium,* Baltimore, USA, 1 – 4.

Saha, C. and Siddiqui, J. Y. (2011). A comparative analyis for split ring resonators of different geometrical shapes. *2011 IEEE Applied Electromagnetics Conference (AEMC),* Kolkata, India, 1 – 4.

Sato, Y., Ogura, N., Yamaguchi, Y., and Ju, Y. (2021). Development of a sensor for dielectric constant measurements utilizing time-domain measurement with a vector network. *Measurement,* 169, 108530.

Shahzad, W., Hu, W. D., Samad, A., and Ligthart, L. P. (2020). Complementary Split Ring Resonator based Metamaterial sensor for Dielectric Materials Measurements. 2*020 17th International Bhurban Conference on Applied Sciences and Technology (IBCAST),* Islamabad, Pakistan, 695 – 698.

Shin, H. J., Oh, S. J., Lim, M. –C., Choi, S. –W., and Ok, G. (2018). Dielectric traces of food materials in the terahertz region. *Infrared Physics & Technology,* 92, 128 – 133.

Singh, J., Jha, S. K., Singh, V., Awasthi, Y. K. (2021). Design of THz low pass filter using split-ring resonators. *Optik,* 247, 167925.

Szostak, K. and Slobodzian, P. (2018). Broadband Dielectric Measurement of PCB and Substrate Materials by Means of a Microstrip Line of Adjustable Width. *IEEE Microwave and Wireless Components Letters,* 28(10), 945 – 947.

Tiwari, N. K., Jha, A. K., Singh, S. P., Akhter, Z., Varshney, P. K., and Akhtar, M. J. (2018). Generalized Multimode SIW Cavity-Based Sensor for Retrieval of Complex Permittivity of Materials. *IEEE Transactions on Microwave Theory and Techniques,* 66(6), 3063 – 3072.

Trabelsi, S. and Nelson, S. O. (2008). Microwave dielectric sensing of moisture content in shelled peanuts independent of bulk density and with temperature compensation. *2008 IEEE Sensors Applications Symposium,* Atlanta, USA, 51 – 53.

Turney, S. (2022). Coefficient of Determination (R^2) | Calculation & Interpretation. *Scribbr*. Available at: https://www.scribbr.com/statistics/coefficient-of-determination (Accessed: 30 September 2022).

Venkatesh, M. S. and Raghavan, G. S. V. (2005). An overview of dielectric properties measuring techniques. *Canadian Biosystems Engineering*, 47, 15 – 30.

Wang, C., Liu, X., Gan, L., and Cai, Q. (2021). A Dual-Band non-destructive Dielectric Measurement Sensor Based on Complementary Split-Ring Resonator. *Front. Phys*, 9:669707, 11 – 20.

Wang, D. and Dang, Z. M. (2018). 12 - Processing of Polymeric Dielectrics for High Energy Density Capacitors. *William Andrew Publishing*, 429 – 446.

Yamaguchi, Y. and Sato, Y. (2017). Measuring method of complex dielectric constant with monostatic horn antenna in W-band using multiple distance measurements and analysis. *2017 IEEE Asia Pacific Microwave Conference (APMC)*, Kuala Lumpur, Malaysia, 666 – 669.

Yaw, K. C. (2012). Measurement of Dielectric Material Properties. *Rohde & Schwarz Regional Headquarters Singapore Pte. Ltd.*

Zeng, N., Li, J., Igbe, T., Liu, Y., Yan, C., and Nie, Z. (2018). Investigation on Dielectric Properties of Glucose Aqueous Solutions at 500 KHz-5MHz for Noninvasive Blood Glucose Monitoring. *2018 IEEE 20th International Conference on e-Health Networking, Applications and Services (Healthcom)*, Ostrava, Czech Republic, 1 – 5.